The role of hydrogen bonding in peptoid-based marine antifouling coatings.

Mikayla E. Barry,[†, Δ] Emily C. Davidson,[‡, Δ] Chengcheng Zhang, [§] Anastasia L. Patterson,[†] Beihang Yu,[‡] Amanda K. Leonardi,[//] Nilay Duzen,[#] Ketaki Malaviya,[‡] Jessica L. Clarke,[⊥] John A. Finlay,[⊥] Anthony S. Clare,[⊥] Zhan Chen, [§] Christopher K. Ober,[#//] and Rachel A. Segalman.[*,†, ‡]

[†]Materials Department and [‡]Department of Chemical Engineering, University of California, Santa Barbara, Santa Barbara, California 93106, United States;

[§]Department of Chemistry, University of Michigan, Ann Arbor, Michigan 48109, USA;

[⊥]School of Marine Science and Technology, Newcastle University, Newcastle upon Tyne NE17RU, U.K.;

[//]Department of Chemistry and Chemical Biology and [#]Department of Materials Science and Engineering, Cornell University, Ithaca, New York 14853, United States

[Δ]Both authors contributed equally to this work.

*E-mail: segalman@engineering.ucsb.edu (R.A.S).

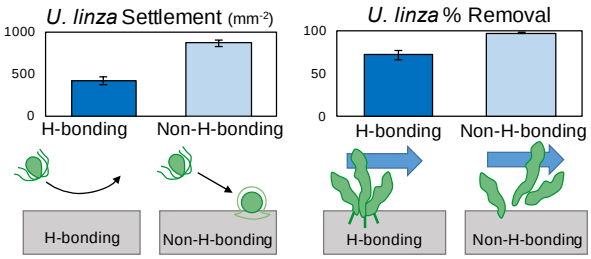

Abstract

The benefits of incorporating amphiphilic properties into antifouling and fouling-release coatings is now well-established. The use of sequence-defined peptides and peptoids in these coatings allows for precise control over the spacing and chemistry of amphiphilic groups, but amphiphilic peptoids have generally outperformed analogous peptides for reasons attributed to differences in backbone structure. The present work demonstrates that the superior properties of peptoids relative to peptides is primarily attributable to a lack of hydrogen bond donors rather than to the secondary structure. A new amphiphilic peptoid was designed containing functional groups similar to those typically found on a hydrogen-bonding peptide backbone. The properties of the peptide were compared with those of a non-hydrogen-bonding peptoid analogue, and both were incorporated as side chains in PDMS-based polymer scaffolds. Bioassays with the soft algal

fouling organisms *Ulva linza* and *Navicula incerta* indicated that hydrogen bonding largely determines the differences seen between similar peptide and peptoid species, while sum frequency generation vibrational spectroscopy suggests that the presence of hydrogen bond donors enhanced interfacial water structuring. This reduced initial *U. linza* adhesion, but the attached algae were more strongly bound by hydrogen-bonding interactions. Consequently, amphiphilic materials lacking hydrogen bond donors best resist marine fouling.

1. Introduction

Marine fouling, caused by the attachment of a broad range of organisms to marine structures including ships' hulls and offshore rigs, begins soon after exposure to an oceanic environment. The initial changes to the surface are due to chemical conditioning, but this is quickly followed by colonization with unicellular organisms such as bacteria, algae (often predominantly diatoms), fungi and protozoa. Simultaneously, larger organisms begin to attach, including hard calcareous fouling organisms such as tubeworms and barnacles and larger algae such as species of *Ulva*. The presence of these organisms dramatically increases surface roughness and reduces hydrodynamic efficiency for ocean-going vessels.[1-4] Fouling by soft algal slimes requires ship power output to be increased over 20% to maintain cruising speed, and even moderate settlement of calcareous fouling organisms can double the power necessary for transport.[5] Coatings containing biocides, such as copper or tri-*n*-butyltin (TBT), have historically been used to limit the settlement and growth of fouling organisms.[2, 6] However, organotins have since been banned by the International Maritime Organization due to their toxicity to marine life,[2, 7] and other metal-containing biocides are already heavily regulated due to environmental risks.[2, 8] Consequently, there is significant interest in developing biocide-free antifouling materials.[6, 9]

Nontoxic fouling-resistant coatings interfere with the adhesion of fouling organisms via two mechanisms. Antifouling materials, such as those incorporating poly(ethylene oxide) PEO or zwitterions, operate by preventing initial adhesion of the organisms.[3, 10-11] In contrast, organisms can attach to fouling-release materials, such as those containing fluoropolymers and polydimethylsiloxane (PDMS), but only weakly; the polymer's low modulus and low surface energy enhance removal of fouling organisms by hydrodynamic forces.[2-3, 12] Many different materials have been tested, but siloxane coatings containing silicone oil lubricants in particular have shown excellent fouling-release properties.[13-14] Another approach is to include amphiphilic

groups in the coatings where it has been shown that the combination of hydrophilic and hydrophobic components at the surface can be particularly effective in minimizing permanent attachment.[15-17] A wide variety of chemical structures have been used in these amphiphilic materials and can be found in a number of reviews.[3, 10, 18-19] However, comparison of the functional groups that provide these amphiphilic materials with their antifouling properties is difficult, as amphiphilic materials are known to induce varying responses depending on the length scale of the hydrophilic and hydrophobic components as well as the components' chemical identities.[20-22]

The incorporation of unique amphiphilic groups into surface-active block copolymers (SABCs) is an effective framework for studying the antifouling and fouling-release properties of selected chemistries.[21, 23-25] Chemical functionalities can be attached via click chemistry as side chain substituents in a block copolymer, allowing for direct comparison of a number of functional groups on a single, unchanging polymer scaffold. Full coatings can also be produced that consist of a thin layer of SABC above commercially-available polystyrene-*b*-poly(ethylene/butylene)-*b*-polystyrene (SEBS), which allows for surface chemistries to be varied without compromising mechanical stability or altering the polymer modulus. Perhaps most importantly, minimal amounts of surface-active functionalities incorporated into only the top layer of the coating can be used to significantly alter surface properties and antifouling characteristics. This system has been used to independently investigate the roles played by amphiphile chemistry,[25] moiety patterning,[21] and block copolymer framework identity[23] on antifouling and fouling-release profiles.

Precise control over the length scale between a wide range of modular amphiphilic components can be attained in these SABCs with the use of peptoids, sequence-defined peptidomimetic *N*-substituted glycine oligomers. An iterative synthesis of sub-monomer units allows for control of monomer type in defined sequences along the peptoid chain.[26-27] Because the formation of the amide group in each peptoid monomer is divided into two reactions, virtually any primary amine can be incorporated into the chain, with a higher yield per reaction that allows for increased

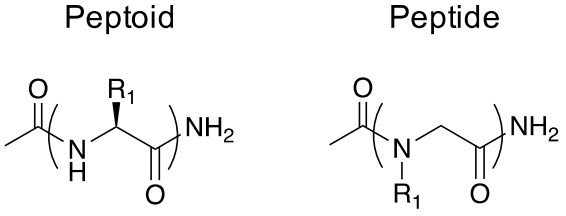

Figure 1. Peptoid N-substitution changes the backbone structure relative to peptides,

(gram-scale) batch size, relative to peptides, and polymeric chain lengths. Furthermore, *N*-substitution in peptoids results in a tertiary amide that inherently lacks hydrogen bond donors, unlike the secondary amides present in peptides, and eliminates the chirality of the backbone α-carbon that enables secondary structure in peptides (**Figure 1**).

SABCs leveraging amphiphilic peptoids as side chains have been shown to reduce fouling through both antifouling and fouling-release methods.[20, 22] However, amphiphilic peptides have not demonstrated the same degree of success for marine fouling applications: peptide side chains on modified poly(dimethylsiloxane) (PDMS) block copolymer coatings have been shown to have higher attachment of *Navicula incerta* and significantly reduced surface-release efficacy for *Ulva linza* relative to coatings modified with analogous peptoid side chains.[22] Despite their similar chemical structure (**S.I. Figure S1**), the peptide-containing samples also demonstrated significantly reduced *U. linza* settlement. Because analogous pendant groups were used for the peptoid and peptide side chains, the contrasting fouling behavior was attributed to differences between the peptide and peptoid backbones (**Figure 1**).

To better understand the role of hydrogen bonding in antifouling and fouling-release performance, a new hydrophilic peptoid monomer was developed that included a hydrogen-bond-donating amide group, which was added to the hydrophilic moiety from previously-tested amphiphilic peptoids.[22] Amphiphilic peptoids containing either this hydrogen-bonding monomer or a non-hydrogen-bonding analogue were incorporated into PDMS-based SABCs (**Figure 2**) to determine the effects of hydrogen bonding on the attachment and release of fouling algae. Further surface characterization performed via sum-frequency generation (SFG) vibrational spectrosocpy suggests a competing hydration-based mechanism for differences in performance.

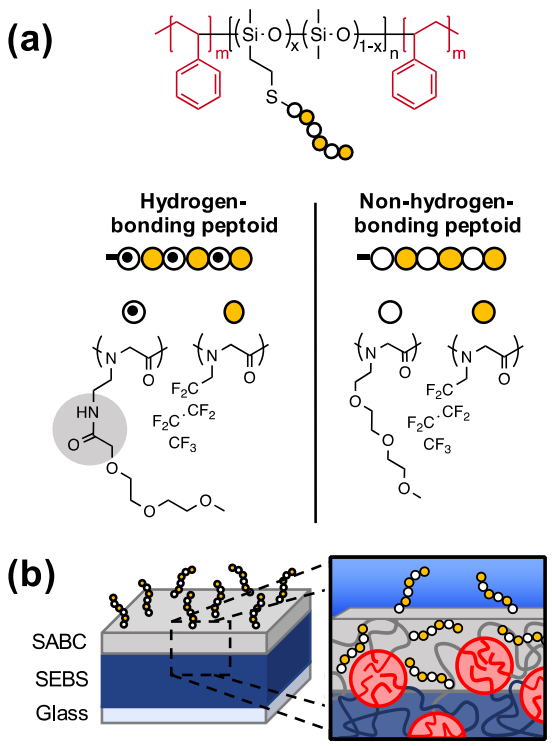

Figure 2. (a) Analogous hydrogen-bonding or non-hydrogen-bonding pendant groups were incorporated into amphiphilic peptoid side chains on a PDMS-based surface-active block copolymer (SABC). **(b)** Samples consisted of a spray-coated SABC on a spin-coated SEBS underlayer to form the final coating. Annealing enabled diffusion between PS microphase-segregated spheres in both layers, lending mechanical stability to the final coating.

2. Experimental Section

Materials

All materials were purchased from Sigma-Aldrich and used as received, unless otherwise noted. Polystyrene-*block*-poly(ethylene-*ran*-butylene)-*block*-polystyrene (SEBS, MD6945) and maleic anhydride-grafted SEBS (MA-SEBS, FG1901X) were generously provided by Kraton Polymers. Hexamethylcyclotrisiloxane (D3) was purchased from Gelest. Boc-ethylene diamine, Boc-ethanolamine, and S-trityl-3-mercaptopropionic acid were purchased from Oakwood Chemicals. Basic alumina and 2,2-dimethoxy-2-phenylacetophenone (DMPA) were obtained from Acros Organics, and triethylene glycol monomethyl ether was purchased from Fluka Analytical. Bromoacetic acid was purchased from Alfa Aesar and dichloromethane was purchased from Fisher Scientific. Dimethylformamide (DMF) was purchased from VWR, diisopropylcarbodiimide was purchased from Chem-Impex, and Rink amide MBHA resin (0.80 mmol/g) was purchased from Millipore Sigma. 1H,1H-perfluoropentylamine was purchased from Manchester Organics,

and triisopropylsilane (TIS) was purchased from TCI. Dry tetrahydrofuran used in synthesis was purified by solvent columns (PureSolv) from Innovative Technology, Inc.

Tetrahydrofuran (THF) and styrene for anionic polymerization of polystyrene-*block*-poly(dimethylsiloxane-*ran*-vinylmethylsiloxane)-*block*-polystyrene (PS-*b*-P(DMS/VMS)-*b*-PS) were dried by stirring over ground calcium hydride (CaH_2), then distilled and degassed by a freeze–pump–thaw process. 1,3,5-trivinyl-1,3,5-trimethylcyclotrisiloxane (V3) was dried by stirring over CaH_2 at 40 °C, then distilled and degassed by a freeze–pump–thaw process. Hexamethylcyclotrisiloxane (D3) was dried by stirring in benzene over CaH_2, distilled, and then sublimed into a flask containing benzene and dried styrene polymerized with *sec*-butyl lithium. Continued stirring further dried the D3 until the solution was colorless, after which the benzene was distilled and the D3 sublimed into a clean flask. Any remaining benzene was distilled off, leaving dried trimer. Dichlorodimethylsilane and chlorotrimethylsilane were purified by distillation and degassed by sparging with N_2.

PS-b-P(DMS/VMS)-b-PS synthesis

PS-*b*-P(DMS/VMS)-*b*-PS synthesis followed an established procedure previously reported.[22] In brief, polystyrene was polymerized with *sec*-butyl lithium and chain-extended with distributed polydimethylsiloxane and polyvinylmethylsiloxane. A triblock architecture was made by coupling active chain ends together. The final molecular weight of the polymer was determined by GPC, while 1H-NMR verified vinyl content. Further details can be found in the S.I.

Synthesis of triethylene glycol amine

The non-H-bonding submonomer (**Figure 2a**) was synthesized by a series of displacements on triethylene glycol monomethyl ether ($mPEG_3$-OH). First, $mPEG_3$-OH (88.7 g, 540 mmol) and *N,N*-diisopropylethylamine (DIEA; 83.7 g, 648 mmol) were combined in 160 mL of dry tetrahydrofuran (THF), then cooled to 0 °C and purged with N_2 for 15 minutes. Mesyl chloride (74.3 g, 649 mmol) was added dropwise and left to stir overnight to form the mesylated triethylene glycol amine intermediate. The white filtrate was removed and the reaction solution filtered through silica to separate the desired product. THF was then removed via rotary evaporation and the product redissolved in dimethylsulfoxide. Potassium phthalimide (120 g, 648 mmol) was added and allowed to react overnight. The phthalimide-protected triethylene glycol amine product was extracted into ether and purified using a basic alumina column with

ethyl acetate as the eluent. Solvent was removed by rotary evaporation, yielding a viscous yellow liquid.

The final submonomer product was obtained by deprotecting the phthalimide group with excess butylamine. A portion of the phthalimide $mPEG_3$ (5.83 g, 19.9 mmol) was dissolved in 60 mL of ethanol. Butylamine (3.93 mL, 39.8 mmol) was added and the reaction was stirred overnight at 70 °C. The solids were removed by filtration, and ethanol and excess butylamine were then evaporated under reduced pressure at room temperature. The crude product was redissolved in chloroform and extracted into 0.6 M aqueous HCl. The amine was then neutralized with 0.5 M NaOH, extracted back into chloroform, and dried with $MgSO_4$. Rotary evaporation then yielded the pure submonomer product, confirmed by ^1H NMR and UPLC-MS. Notably, this synthesis route avoids the use of either sodium azide or hydrazine.

Synthesis of amide-linked triethylene glycol amine

The hydrogen-bond-donating submonomer (**Figure 2a**) was synthesized using DIC-mediated coupling of a triethylene glycol carboxylic acid and Boc-protected diamine. 2-[2-(2-Methoxyethoxy)ethoxy]acetic acid ($mPEG_3$-COOH; 80.9 g, 421 mmol) was dissolved in 500 mL DMF, then *N,N'*-diisopropylcarbodiimide (DIC; 71.1 mL, 454 mmol) was added and allowed to stir for 30 minutes. *N*-Boc-ethylenediamine (87.3 g, 545 mmol) in 300 mL DMF was then added. The reaction was purged with N_2 and allowed to run overnight. DMF was removed via centrifugal evaporation and solid DIC byproducts were filtered out. The Boc-protected amide-linked $mPEG_3$ amine product was purified using an alumina plug with ethyl acetate as eluent.

The protected amide-linked amine was deprotected using trifluoracetic acid (TFA). 10 g of protected amine (31 mmol) were dissolved in 60 mL DCM. TFA (40 mL, 522 mmol) was added dropwise and allowed to stir for 2.5 hours, at which time thin layer chromatography confirmed complete removal of the protecting group. DCM and TFA were then removed under reduced pressure. The deprotected amide-linked amine was next dissolved in water and washed three times with DCM and once with ether. Water was removed using rotary evaporation. The charged terminal amine was then neutralized by dissolving the deprotected amine product (6 g, 27 mmol) in 1 M DMF solution (27 mL), and slowly adding 1:1 NaOH:H_2O (w/v) solution, stirring until neutral pH was reached.[28] The submonomer identity was confirmed via UPLC-MS before the neutralized 1 M DMF solution was used in peptoid synthesis.

Peptoid synthesis

Peptoids were synthesized on a Prelude synthesizer (Protein Technologies) according to published solid-phase submonomer synthesis procedures using Rink amide MBHA resin.[20, 22, 26] Two sequences of hexamer peptoids were made, one with three alternating 1*H*,1*H*-perfluoropentylamine submonomers and three triethylene glycol submonomers, while the other contained alternating fluorinated submonomers and amide-linked triethylene glycol submonomers. The *N*-terminus of the peptoid chain was capped with *S*-trityl-3-mercaptopropionic acid that, upon cleavage and deprotection with trifluoroacetic acid, yielded a thiol-terminated oligomer capable of attachment to the PDMS-based polymer via a radical mediated thiol–ene "click" reaction. The cleaved peptoids were dissolved in a 1:1 acetonitrile:water (v/v) solution and washed with hexanes, then lyophilized to yield the pure peptoid product as confirmed by UPLC-MS (**S.I. Figure S2**). Further synthetic details can be found in the S.I.

Click attachment to polymer scaffold

Thiol-terminated peptoids were incorporated into the siloxane triblock copolymer via radical mediated thiol–ene "click" chemistry as previously reported.[22] Triblock copolymer (0.95 g, 0.3 mmol vinyl groups) was dissolved in 10 mL of dichloromethane, to which either the H-bonding peptoid (2.3 g, 1.3 mmol) or non-H-bonding peptoid (2.2 g, 1.4 mmol) were added. After adding 65 mg of 2,2-dimethoxy-2-phenyl acetophenone (DMPA), the solution was sparged with N_2 for 30 min, then irradiated with 365 nm UV light while stirring for 3 h. The peptoid-modified PDMS triblock copolymer was then precipitated into methanol, filtered, and dried under vacuum. ^{1}H NMR verified a 75% reduction of vinyl peaks for both materials, likely limited by steric hindrance associated with substituting three sites per V3 monomer unit with peptoid side chains (**S.I. Figure S5**).

Slide preparation for biofouling assays

Coated slides for *U. linza* and *N. incerta* assays were prepared as previously reported. Microscope glass slides (3 x 1 in) were cleaned using nanostrip for 30 minutes, then rinsed sequentially with deionized water and anhydrous ethanol. After drying, the clean glass slides were aminosilane-treated by soaking overnight in dilute 3-(aminopropyl)trimethoxysilane solution (3.5% in anhydrous ethanol (v/v)) with a catalytic amount of acetic acid. The slides were then sequentially rinsed with anhydrous ethanol and water, then cured in vacuum at 120 °C for 4 h. Immediately after curing, the slides were spin-coated with an initial SEBS/MA-SEBS

solution (7% SEBS (w/v) and 2% MA-SEBS (w/v) in toluene) at 500 rpm for 5 s, followed by 2500 rpm for 30 s. Curing at 120 °C under vacuum for 24 h enabled the maleic anhydride groups on the polymer backbone to react with amine groups on the functionalized glass surface, improving adhesion strength between the polymer and glass. An additional SEBS solution (12% SEBS in toluene (w/v)) was then applied via spin-coating three times (2500 rpm, 30 s). The 1 mm thick coating was then annealed under vacuum at 120 °C for 24 h. H-bonding, non-H-bonding, and unfunctionalized PDMS-based SABC solutions (5% w/v in 20:1 DCM:toluene (v/v)) were spray-coated (Badger model 250 airbrush) on SEBS-coated slides to form a top layer tens of microns thick. Annealing at 60 °C for 6 h and then 120 °C for 24 h allowed for diffusion of the microphase-segregating PS groups between layers, improving mechanical stability.

Prism preparation for SFG study

For SFG testing, optically clear CaF_2 prisms were cleaned via ozone treatment and spin-coated with sample solutions to sufficient thickness to ensure sample signal solely came from the material–environment interface, determined experimentally to be at least 50 nm (**S.I. Figure S7**). Due to solubility differences, the unfunctionalized PDMS-based SABC solution (2.5 wt% in cyclohexane) was applied once (1500 rpm, 45 s) while the H-bonding and non-H-bonding SABCs (1 wt% in cyclopentanone) were applied twice (1000 rpm, 2 min). Thickness was confirmed via ellipsometry on corresponding silicon substrates to be between 50 and 200 nm.

^{1}H NMR

All ^{1}H NMR spectra were obtained using a Varian VNMRS 600 MHz spectrometer in $CDCl_3$ solution.

UPLC-MS

Mass data for all samples were obtained using a Waters Acquity H-class Ultra High Pressure Liquid Chromatography (UPLC) system coupled with a Waters Xevo G2-XS Time-of-Flight Mass Spectrometer. Time-of-flight mass spectrometry was obtained in positive electrospray ionization (ESI^+) mode. Liquid chromatography separations used gradients from H_2O to ACN with 0.1% TFA on a BEH C_{18} column.

Water contact angle

Water contact angles were measured using the captive bubble method. In summary, sample slides were suspended in Milli-Q water with the coated side facing down. A 22-gauge stainless

steel needle was used to release a bubble that was trapped against the coated face of the sample. This provided contact angle measurements under full immersion, which more closely replicates the underwater conditions experienced by antifouling materials. For each material, the contact angle was measured in triplicate (in different locations) for three separate slides. To characterize film restructuring underwater, contact angle measurements were taken immediately after submersion, after 5 h, and then every 24 h over the course of 7 days. All measurements were collected using the ramé-hart model 100-00 goniometer.

Ulva linza *bioassays*

Before performing *U. linza* biofouling assays, nine coated slides for each material were equilibrated for 72 hours in 0.22 μm filtered artificial seawater (ASW, Tropic Marin) in individual wells of quadriPERM dishes (Sarstedt). Zoospores were obtained from mature plants according to a standard method,[29] then suspended in a solution of filtered ASW at a concentration of 1×10^5 mL^{-1}. 10 mL of the suspension was added to each well of the quadriPERM dishes and allowed to settle in darkness for 45 min at 20 °C. Unsettled spores were then removed by gently washing in filtered ASW. Three slides were set aside, fixed using 2.5% glutaraldehyde in ASW, and analyzed to determine spore settlement density using a Zeiss Axioskop 2 fluorescence microscope. Leica LASX image analysis software was used to count 30 fields of view of 0.15 mm^2 on each slide.

The spores on the remaining six slides were cultured for 7 days in an illuminated incubator using nutrient-supplemented ASW to produce sporelings (young plants). Sporeling biomass was determined *in situ* by chlorophyll fluorescence measurements using a Tecan fluorescence plate reader (GENios Plus), and quantified in terms of relative fluorescence units (RFU) determined as the mean of 70 point fluorescence readings taken from the central portion of each slide.

Sporeling attachment strength was assessed by determining biomass removal after using a water jet to spray the surface with an impact pressure of 55 kPa.[30] The biomass remaining on the sample was again quantified using the fluorescence plate reader, and the percentage removal calculated from the difference in biomass RFU before and after exposure.

Navicula incerta *bioassays*

Before performing *N. incerta* assays, six coated slides for each material were equilibrated for 72 hours in 0.22 μm filtered ASW in individual wells of quadriPERM dishes. *N. incerta* cells were

cultured for 3 days, then diluted to produce a suspension with chlorophyll *a* content of approximately 0.25 μg mL^{-1}. Ten mL of the suspension was then added to each quadriPERM well and left to settle for 2 h at 20 °C. Unbound cells were removed by shaking on an orbital shaker at 60 rpm for 5 minutes, followed by rinsing in seawater. Three slides were set aside, fixed in 2.5% glutaraldehyde in ASW, air dried, and then analyzed via transmitted light microscopy to quantify initial attachment density. Manual counts were made for 15 fields of view of 0.15 mm^2 per slide.

Diatom attachment strength was then determined for the remaining three slides by quantifying removal after exposure to a shear stress of 28 Pa in a specially-designed water channel.[31] The diatoms were fixed by immersing the slides in glutaraldehyde solution (2.5% (v/v) in ASW) and cells counted using transmitted light microscopy as before.

Statistical Analysis

U. linza settlement and *N. incerta* initial attachment data are presented as means with 95% confidence intervals and were analyzed via one-way ANOVA to identify statistically significant differences between groups ($p < 0.05$), followed by a post hoc pairwise Tukey comparison test. Percent removal for *U. linza* and *N. incerta* is presented as means within 95% confidence intervals and the statistical tests previously mentioned were used to analyze the arcsine transform of fractional removal data.

SFG Testing

Sum-frequency generation (SFG) theory, experimental details, and data analysis have been extensively reported,[32-41] and spectra of the coated prisms were collected in air and water according to previously reported methods.[35-41] SFG data collection used two input laser beams, a visible beam and an infrared beam, both with a diameter of approximately 0.5 mm. The visible beam, with a fixed wavelength at 532 nm, was generated by doubling the frequency of a 20 ps pulse width output from an EKSPLA Nd:YAG laser. The IR beam with wavenumber tunability from 1000 to 4300 cm^{-1} was produced using an EKSPLA optical parametric generation/amplification and difference frequency generation system with LBO and $AgGaS_2$ crystals. These two input beams penetrated the prism and then reached the polymer coating surfaces that were in contact with either air or water, superimposed on each other spatially and temporally to generate the sum frequency (SF) signal. This signal was collected using a

photomultiplier and net intensity normalized by measuring the input visible and IR intensities according to the back reflections of the two beams using the focus lenses.

3. Results and Discussion

The hydrogen-bonding (H-bonding) peptoid and its non-hydrogen-bonding (non-H-bonding) peptoid analogue were individually incorporated into triblock SABCs consisting of a PDMS-based midblock with polystyrene (PS) end blocks (**Figure 2a**). Each sample consisted of a SABC topcoat above a layer of a SEBS thermoplastic elastomer to provide a consistent modulus in the material and improve the coating's mechanical stability. Annealing enabled the microphase-separated PS end blocks to diffuse between the SABC and SEBS layers, forming physical anchors that prevent delamination (**Figure 2b**). The samples were evaluated for fouling resistance and release using *U. linza* and *N. incerta* bioassays and were characterized using captive bubble water contact angle measurements and sum-frequency generation. In addition to the H-bonding and non-H-bonding peptoid samples, the unfunctionalized PDMS-based polymer scaffold served as a control to identify the effects of amphiphilicity on surface properties and fouling.

The H-bonding amphiphilic peptoid was designed to act as a hydrogen-bonding peptide mimic without the structural effects caused by chirality. Because the peptoid backbone innately lacks hydrogen bonding, a secondary amide (as the source of hydrogen-bonding in the peptide backbone) was added along the side chain in the ether-based hydrophilic monomer. The amphiphilic peptoid was made by alternating this hydrogen-bonding monomer with a hydrophobic peptoid monomer containing fluoralkyl functionality.

The surface activity of both amphiphilic peptoid side chains was confirmed using captive bubble contact angle goniometry, chosen over conventional contact angle goniometry to better mimic the underwater environment experienced by surfaces exposed to biofouling organisms. The H-bonding and non-H-bonding peptoid materials both demonstrated increased hydrophilicity relative to the unfunctionalized PDMS-based control (**S.I. Figure S6**). Notably, the contact angle of the two peptoid-containing samples approached similar values over extended time underwater, suggesting the equilibrated surfaces maintained comparable surface energy and hydrophilicity.

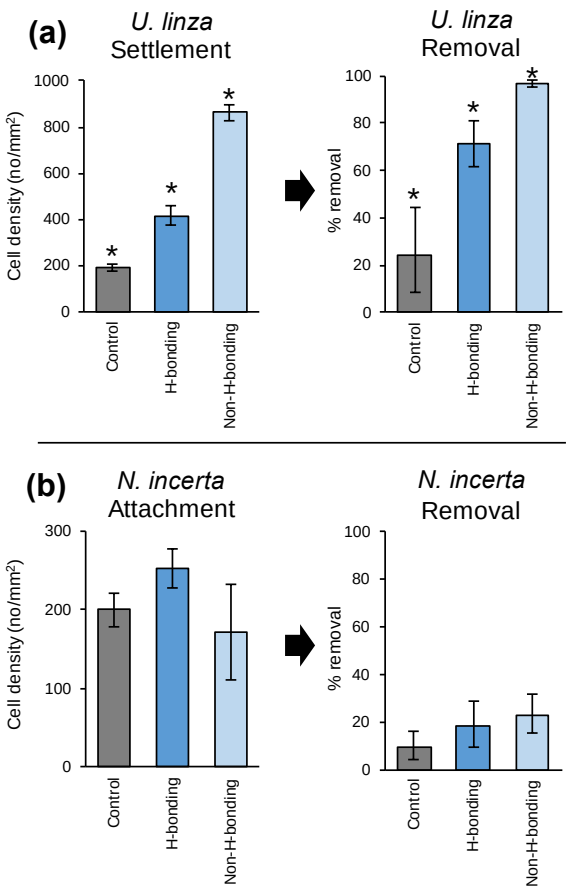

Figure 3. Biofouling assay settlement and release data for peptoid-modified PDMS and the unfunctionalized PDMS-based polymer control. **(a)** Fouling results for *U. linza* indicate the H-bonding sample minimizes settlement relative to its non-H-bonding analogue, but demonstrates inferior fouling-release compared with the non-hydrogen-bonding sample. All samples differ significantly (*$p<0.05$). **(b)** Fouling results for *Navicula incerta* indicate minimal effects due to the presence of amphiphilic peptoid chains; the PDMS scaffold dominated behavior. Error bars on all data indicate 95% confidence limits.

Despite their similar hydrophilicity, the peptoid materials differed greatly in antifouling and fouling-release properties in *U. linza* bioassays (**Figure 3a**). The settlement of *U. linza* spores was much higher on the non-H-bonding peptoid than on either the PDMS-based scaffold control or the H-bonding surface ($F_{2,267} = 421.7$; $p<0.05$). When subjected to a water jet with impact pressure of 55 kPa, the same non-H-bonding surface demonstrated nearly perfect removal. releasing over 97% of the sporelings present on its surface, ($F_{2,15} = 40.9$; $p<0.05$). The 7-day-old sporelings were particularly weakly attached to this coating as a result of the chemistry and spacing of its hydrophilic and hydrophobic functionalities. The extremely high level of removal resulted in a far cleaner surface than those of the other two materials ($F_{2,15} = 27.9$; $p<0.05$ (**Figure 4**).

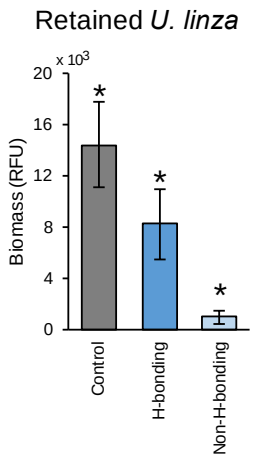

Figure 4. High removal rates of *U. linza* for the non-H-bonding sample significantly reduced retained sporelings (*p<0.05) relative to the H-bonding and unfunctionalized PDMS materials. Error bars indicate 95% confidence limits.

U. linza tends to attach strongly to moderately hydrophilic materials such as glass.[42-43] The findings of this study suggest that attachment of spores of *U. linza* to surfaces may be strongly influenced by hydrogen bonding. The introduction of hydrogen bonding in the H-bonding peptoid did not alter macroscale hydrophilicity relative to its non-H-bonding analogue (see **S.I. Figure S6** for contact angle comparisons) but did increase the attachment strength of *U. linza* sporelings. The biomass remaining on each surface after exposure to the shear stress is shown in **Figure 4**. The H-bonding peptoid surface retained over 28% of sporelings, leaving nearly eight times the fouling present on the non-H-bonding peptoid film. Although the H-bonding peptoid surface showed lower settlement compared with the non-H-bonding peptoid film, its fouling-release properties were not as good, making it less useful for practical applications.

While the PDMS-based scaffold control had lower settlement than either amphiphilic peptoid sample, adhered sporelings were more strongly bound and the surface retained the most fouling after removal. As had been seen before,[22] modification with amphiphilic peptoids appears to improve fouling-release properties, though the extent of success varied. We consequently conclude that the non-H-bonding sample better resists permanent *U. linza* attachment compared with both its H-bonding analogue and the PDMS control.

In contrast to *U. linza,* hydrogen bonding did not appear to drive or hinder fouling by *N. incerta* relative to the effects of the scaffold material (**Figure 3b**). Initial attachment was lower on the non-H-bonding surface than on the H-bonding one, but neither were significantly different to the PDMS scaffold ($F_{2,134}$ = 4.3; $p<0.05$). There was no difference in removal from the three surfaces when exposed to a shear stress of 28 Pa ($F_{2,132}$ = 1.3; $p>0.05$) and fouling release was relatively low under this flow regime. Previous work has indicated that the initial attachment of diatoms depends largely on the properties of the SABC into which the peptoid side chains are incorporated. This has been demonstrated in the superior performance of poly(ethylene oxide)-based peptoid coatings compared to their PDMS-based counterparts.[22] As a result, the similarities between samples can be attributed to the scaffold polymer rather than the H-bonding and non-H-bonding peptoid side chains.

The results for *U. linza* and *N. incerta* correlate with those seen in previous experiments using peptides and peptoids;[22] while settlement of *U. linza* spores was higher on the non-H-bonding peptoids, the same coatings showed superior fouling-release efficacy and ultimately better resistance to permanent adhesion. Because the H-bonding and non-H-bonding materials maintained similar macroscale hydrophilicity, the presence of peptide-like hydrogen bond donors must result in a microscale physicochemical change that substantially alters the underwater interface and its interactions with fouling organisms.

The chemical structure of surfaces can be investigated using sum frequency generation (SFG) vibrational spectroscopy, a second-order nonlinear optical spectroscopic technique.[32-34, 44-48] The surface sensitivity of the SFG spectroscopy comes from its selection rule, wherein only a medium with no inversion symmetry can generate SFG signal. Because symmetry is broken at surfaces and interfaces but not in the bulk, SFG signals can be generated with surface specificity in the topmost surface layer.[49] SFG has been developed into a powerful tool to investigate many surfaces and interfaces, including polymer surfaces in water.[35-41]

SFG surface analysis of the H-bonding and non-H-bonding peptoid materials underwater indicates that water binding strength may be responsible for the observed differences in fouling behavior for *U. linza* (**Figure 5**).

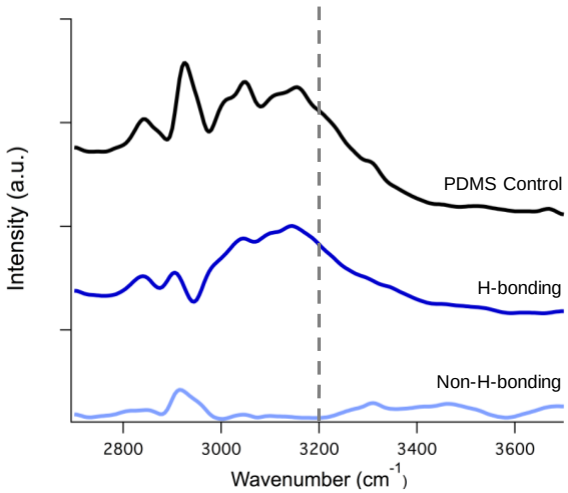

Figure 5. SFG spectra taken underwater show varying intensities for strong water bonding at 3200 cm^{-1} as indicated by the dashed line. The H-bonding sample and PDMS control both show highly ordered water at the interface, while the non-H-bonding sample shows little ordering. Spectra are vertically offset for clarity.

Strongly hydrophilic or hydrophobic surfaces can induce the organization of water molecules near the surface into strongly ordered structures, where interfacial water molecules align and therein emit strong SFG signals.[50-52] This tightly bound, strongly ordered water is visible as broad peaks centered near 3200 cm^{-1} for the H-bonding peptoid and the PDMS-based control (lacking peptoid side chains), but not for the non-H-bonding peptoid. These findings could explain the reduced settlement of *U. linza* on the H-bonding peptoid, as tightly bound water partially shields the surface from spores. However, upon displacement of the water followed by *U. linza* settlement and growth, stronger interactions between the organism and the surface are high enough to resist removal. Conversely, the non-H-bonding peptoid that lacked water structuring showed higher *U. linza* settlement, but the sporelings were only weakly bound to the surface as indicated by its 97% fouling release.

The formation of a structured water layer for the H-bonding peptoid material but not for its non-H-bonding analogue seems to be due primarily to hydrogen bond donation rather than differences in surface energy, as contact angle results indicate similar hydrophilicity between peptoid materials, while the non-functionalized control had increased hydrophobicity (**S.I. Figure S6**), and SFG spectroscopy indicates both peptoid chains were present at the surface in water (**S.I. Figure S8**). Many antifouling coatings rely on the presence of a hydration layer to prevent settlement of proteins or cells, but, in this system, the strength of this hydration layer may come at the cost of increased affinity for some fouling species such as *U. linza*.

Interestingly, the hydrophobic PDMS control showed high ordering of water despite lacking hydrophilic groups, but similar hydrophobic surfaces have already been shown to enhance water ordering in SFG measurements.[50, 53] Furthermore, the effects of this ordering are similar to those for the H-bonding material: fouling results for *U. linza* show similarly low settlement as well as poor fouling release. Prior work has shown that these amphiphilic peptoid side chains are most successful when used to strengthen the antifouling mechanism of the host polymer. The incorporation of the H-bonding peptoid amphiphile into a PDMS-based scaffold polymer, which is designed for fouling release rather than fouling resistance, reduced *U. linza* settlement at the expense of release. The presence of the non-H-bonding amphiphile, despite having a higher spore settlement density than its H-bonding analogue, enhanced fouling release of *U. linza* sporelings from the PDMS-based scaffold to over 97%. Therefore, the non-H-bonding amphiphile can be considered the superior candidate for resisting fouling algae on fouling-release coatings such as PDMS.

4. Conclusions

Peptoid-based coatings have shown promise in marine antifouling due to their versatility, leveraging control over a large number of chemical functionalities as well as their positions relative to each other. Despite their similar attributes, peptide-containing materials have failed to match the success of their peptoid analogues.[22] The primary cause of this difference was suspected to have been related to the hydrogen bond donor present in the secondary amide on the peptide backbone, but peptide chirality also enables the formation of secondary structures, which have been known to play a role in cell attachment.[5, 54] The development of a hydrogen-bonding peptoid that inherently lacks chirality (and therein secondary structure) allowed the study to focus on the role hydrogen bonding plays in the attachment and release of fouling algae. Results of the biofouling assays carried out with the H-bonding and non-H-bonding peptoids has indicated that hydrogen bonding, rather than secondary structure, largely determined the differences seen between similar peptide and peptoid coating components.

Further characterization of the surface with SFG suggested that H-bonding peptoids are surrounded by a highly-ordered water layer that reduced the settlement density of spores of *U. linza*. However, the attachment strength of the sporelings was stronger on these surfaces than on the non H-bonding surfaces. This suggests that once a spore penetrated the water layer and adhered to the surface, its attachment strength was enhanced by the ability to hydrogen bond.

The surface that lacked H-bonding proved the better fouling-release surface and had a cleaner surface after exposure to hydrodynamic removal forces. Many antifouling coatings are understood to function by the formation of a hydration layer (e.g. PEO-based materials); maximizing hydrophilicity without the use of hydrogen bond donors would be expected to improve the fouling resistance and release of algal species such as *U. linza*. In contrast, the adhesion of diatoms to the peptoid-containing coatings did not appear to be affected by hydrogen bonding and it is likely that attachment was largely determined by the PDMS scaffold polymer. Future studies should be performed to verify whether these findings could also be extrapolated to coatings designed primarily according to antifouling (rather than fouling-release) mechanisms.

Associated Content

Supporting Information

Peptoid and block copolymer synthetic scheme, NMR spectra, GPC traces, contact angle goniometry, additional SFG spectra.

Acknowledgments

The authors gratefully acknowledge financial support by the Office of Naval Research (ONR) from **Awards N00014-17-1-2047**, **N00014-13-1-0633**, **N00014-13-1-0634**, **N00014-16-1-3115**, **N00014-16-1-2960**, **N00014-16-1-2988**, and **N00014-16-1-3125**. M.E.B and A.L.P gratefully acknowledge the National Science Foundation (NSF) for graduate fellowships. The authors also made use of facilities through the Molecular Foundry, a Lawrence Berkeley National Laboratory User Facility supported by the Office of Science, Office of Basic Energy Sciences, U.S. Department of Energy, under Contract DE-AC02-05CH11231. The authors thank Rachel Behrens for assistance with mass spectrometry and gratefully acknowledge the use of shared experimental facilities supported by the NSF MRSEC Program under Award No. DMR 1720256, a member of the NSF-funded Materials Research Facilities Network.

Author Information

Corresponding Author

Email: segalman@ucsb.edu (R.A.S)

Present Addresses

E.C.D.: John A. Paulson School of Engineering and Applied Sciences, Wyss Institute for Biologically Inspired Engineering, Harvard University, Cambridge, MA 02138.

Author Contributions

M.E.B and E.C.D. contributed equally to this work.

Notes

The authors declare no competing financial interest.

References

1. Unabia, C. R. C.; Hadfield, M. G., Role of Bacteria in Larval Settlement and Metamorphosis of the Polychaete Hydroides elegans. *Marine Biology* **1999,** *133* (1), 55-64.
2. Chambers, L. D.; Stokes, K. R.; Walsh, F. C.; Wood, R. J. K., Modern Approaches to Marine Antifouling Coatings. *Surface and Coatings Technology* **2006,** *201* (6), 3642-3652.
3. Callow, J. A.; Callow, M. E., Trends in the Development of Environmentally Friendly Fouling-Resistant Marine Coatings. *Nature Communications* **2011,** *2*, 244.
4. Schultz, M. P.; Walker, J. M.; Steppe, C. N.; Flack, K. A., Impact of Diatomaceous Biofilms on the Frictional Drag of Fouling-Release Coatings. *Biofouling* **2015,** *31* (9-10), 759-773.
5. Schultz, M. P., Effects of Coating Roughness and Biofouling on Ship Resistance and Powering. *Biofouling* **2007,** *23* (5), 331-341.
6. Banerjee, I.; Pangule, R. C.; Kane, R. S., Antifouling Coatings: Recent Developments in the Design of Surfaces That Prevent Fouling by Proteins, Bacteria, and Marine Organisms. *Advanced Materials* **2011,** *23* (6), 690-718.
7. Lejars, M.; Margaillan, A.; Bressy, C., Fouling Release Coatings: A Nontoxic Alternative to Biocidal Antifouling Coatings. *Chemical Reviews* **2012,** *112* (8), 4347-4390.
8. Finnie, A. A.; Williams, D. N., Paint and Coatings Technology for the Control of Marine Fouling. *Biofouling* **2010,** *18*.
9. Hellio, C.; Maréchal, J. P.; Da Gama, B. A. P.; Pereira, R. C.; Clare, A. S., Natural Marine Products with Antifouling Activities. In *Advances in Marine Antifouling Coatings and Technologies*, Hellio, C.; Yebra, D., Eds. Woodhead Publishing: 2009; pp 572-622.
10. Yang, W. J.; Neoh, K.-G.; Kang, E.-T.; Teo, S. L.-M.; Rittschof, D., Polymer Brush Coatings for Combating Marine Biofouling. *Progress in Polymer Science* **2014,** *39* (5), 1017-1042.
11. Ekblad, T.; Bergström, G.; Ederth, T.; Conlan, S. L.; Mutton, R.; Clare, A. S.; Wang, S.; Liu, Y.; Zhao, Q.; D'Souza, F.; Donnelly, G. T.; Willemsen, P. R.; Pettitt, M. E.; Callow, M. E.; Callow, J. A.; Liedberg, B., Poly(ethylene glycol)-Containing Hydrogel Surfaces for Antifouling Applications in Marine and Freshwater Environments. *Biomacromolecules* **2008,** *9* (10), 2775-2783.
12. Dobretsov, S.; Thomason, J. C., The Development of Marine Biofilms on Two Commercial Non-Biocidal Coatings: a Comparison Between Silicone and Fluoropolymer Technologies. *Biofouling* **2011,** *27* (8), 869-880.
13. Amini, S.; Kolle, S.; Petrone, L.; Ahanotu, O.; Sunny, S.; Sutanto, C. N.; Hoon, S.; Cohen, L.; Weaver, J. C.; Aizenberg, J.; Vogel, N.; Miserez, A., Preventing Mussel Adhesion Using Lubricant-Infused Materials. *Science* **2017,** *357* (6352), 668-673.
14. Hoipkemeier-Wilson, L.; Schumacher, J. F.; Carman, M. L.; Gibson, A. L.; Feinberg, A. W.; Callow, M. E.; Finlay, J. A.; Callow, J. A.; Brennan, A. B., Antifouling Potential of Lubricious, Micro-engineered, PDMS Elastomers against Zoospores of the Green Fouling Alga Ulva (Enteromorpha). *Biofouling* **2004,** *20* (1), 53-63.
15. Martinelli, E.; Gunes, D.; Wenning, B. M.; Ober, C. K.; Finlay, J. A.; Callow, M. E.; Callow, J. A.; Di Fino, A.; Clare, A. S.; Galli, G., Effects of Surface-Active Block Copolymers with Oxyethylene and Fluoroalkyl Side Chains on the Antifouling Performance of Silicone-Based Films. *Biofouling* **2016,** *32* (1), 81-93.
16. Hawkins, M. L.; Faÿ, F.; Réhel, K.; Linossier, I.; Grunlan, M. A., Bacteria and Diatom resistance of Silicones Modified with PEO-Silane Amphiphiles. *Biofouling* **2014,** *30* (2), 247-258.
17. Gudipati, C. S.; Finlay, J. A.; Callow, J. A.; Callow, M. E.; Wooley, K. L., The Antifouling and Fouling-Release Perfomance of Hyperbranched Fluoropolymer (HBFP)−Poly(ethylene glycol) (PEG) Composite Coatings Evaluated by Adsorption of Biomacromolecules and the Green Fouling Alga Ulva. *Langmuir* **2005,** *21* (7), 3044-3053.

18. Hellio, C.; Yebra, D., *Advances in Marine Antifouling Coatings and Technologies*. Elsevier: 2009.
19. Krishnan, S.; Weinman, C. J.; Ober, C. K., Advances in Polymers for Anti-Biofouling Surfaces. *Journal of Materials Chemistry* **2008,** *18* (29), 3405-3413.
20. van Zoelen, W.; Buss, H. G.; Ellebracht, N. C.; Lynd, N. A.; Fischer, D. A.; Finlay, J.; Hill, S.; Callow, M. E.; Callow, J. A.; Kramer, E. J.; Zuckermann, R. N.; Segalman, R. A., Sequence of Hydrophobic and Hydrophilic Residues in Amphiphilic Polymer Coatings Affects Surface Structure and Marine Antifouling/Fouling Release Properties. *ACS Macro Letters* **2014,** *3* (4), 364-368.
21. Calabrese, D. R.; Wenning, B.; Finlay, J. A.; Callow, M. E.; Callow, J. A.; Fischer, D.; Ober, C. K., Amphiphilic Oligopeptides Grafted to PDMS-Based Diblock Copolymers for Use in Antifouling and Fouling Release Coatings. *Polymers for Advanced Technologies* **2015,** *26* (7), 829-836.
22. Patterson, A. L.; Wenning, B.; Rizis, G.; Calabrese, D. R.; Finlay, J. A.; Franco, S. C.; Zuckermann, R. N.; Clare, A. S.; Kramer, E. J.; Ober, C. K., Role of Backbone Chemistry and Monomer Sequence in Amphiphilic Oligopeptide-and Oligopeptoid-Functionalized PDMS-and PEO-Based Block Copolymers for Marine Antifouling and Fouling Release Coatings. *Macromolecules* **2017,** *50* (7), 2656-2667.
23. Calabrese, D. R.; Wenning, B. M.; Buss, H.; Finlay, J. A.; Fischer, D.; Clare, A. S.; Segalman, R. A.; Ober, C. K., Oligopeptide-Modified Hydrophobic and Hydrophilic Polymers as Antifouling Coatings. *Green Materials* **2017,** *5* (1), 31-43.
24. Weinman, C. J.; Finlay, J. A.; Park, D.; Paik, M. Y.; Krishnan, S.; Sundaram, H. S.; Dimitriou, M.; Sohn, K. E.; Callow, M. E.; Callow, J. A., ABC Triblock Surface Active Block Copolymer with Grafted Ethoxylated Fluoroalkyl Amphiphilic Side Chains for Marine Antifouling/Fouling-Release Applications. *Langmuir* **2009,** *25* (20), 12266-12274.
25. Krishnan, S.; Ayothi, R.; Hexemer, A.; Finlay, J. A.; Sohn, K. E.; Perry, R.; Ober, C. K.; Kramer, E. J.; Callow, M. E.; Callow, J. A., Anti-Biofouling Properties of Comblike Block Copolymers with Amphiphilic Side Chains. *Langmuir* **2006,** *22* (11), 5075-5086.
26. Zuckermann, R. N.; Kerr, J. M.; Kent, S. B.; Moos, W. H., Efficient Method for the Preparation of Peptoids [oligo (N-substituted Glycines)] by Submonomer Solid-Phase Synthesis. *Journal of the American Chemical Society* **1992,** *114* (26), 10646-10647.
27. Zuckermann, R. N., Peptoid Origins. *Peptide Science* **2011,** *96* (5), 545-555.
28. Figliozzi, G. M.; Goldsmith, R.; Ng, S. C.; Banville, S. C.; Zuckermann, R. N., Synthesis of N-substituted Glycine Peptoid Libraries. In *Methods in Enzymology*, Academic Press: 1996; Vol. 267, pp 437-447.
29. Sundaram, H. S.; Cho, Y.; Dimitriou, M. D.; Weinman, C. J.; Finlay, J. A.; Cone, G.; Callow, M. E.; Callow, J. A.; Kramer, E. J.; Ober, C. K., Fluorine-Free Mixed Amphiphilic Polymers Based on PDMS and PEG Side Chains for Fouling Release Applications. *Biofouling* **2011,** *27* (6), 589-602.
30. Finlay, J.; Callow, M. E.; Schultz, M.; Swain, G.; Callow, J., Adhesion Strength of Settled Spores of the Green Alga Enteromorpha. **2002**.
31. Schultz, M. P.; Finlay, J. A.; Callow, M. E.; Callow, J. A., A Turbulent Channel Flow Apparatus for the Determination of the Adhesion Strength of Microfouling Organisms. *Biofouling* **2000,** *15* (4), 243-251.
32. Perry, A.; Neipert, C.; Space, B.; Moore, P. B., Theoretical Modeling of Interface Specific Vibrational Spectroscopy: Methods and Applications to Aqueous Interfaces. *Chemical Reviews* **2006,** *106* (4), 1234-1258.
33. Chen, Z.; Shen, Y. R.; Somorjai, G. A., Studies of Polymer Surfaces by Sum Frequency Generation Vibrational Spectroscopy. *Annual Review of Physical Chemistry* **2002,** *53* (1), 437-465.

34. Shen, Y. R., Optical Second Harmonic Generation at Interfaces. *Annual Review of Physical Chemistry* **1989,** *40* (1), 327-350.
35. Chen, C.; Wang, J.; Chen, Z., Surface Restructuring Behavior of Various Types of Poly(dimethylsiloxane) in Water Detected by SFG. *Langmuir* **2004,** *20* (23), 10186-10193.
36. Hankett, J. M.; Liu, Y.; Zhang, X.; Zhang, C.; Chen, Z., Molecular Level Studies of Polymer Behaviors at the Water Interface Using Sum Frequency Generation Vibrational Spectroscopy. *Journal of Polymer Science Part B: Polymer Physics* **2013,** *51* (5), 311-328.
37. Hankett, J. M.; Lu, X.; Liu, Y.; Seeley, E.; Chen, Z., Interfacial Molecular Restructuring of Plasticized Polymers in Water. *Physical Chemistry Chemical Physics* **2014,** *16* (37), 20097-20106.
38. Wang, J.; Paszti, Z.; Even, M. A.; Chen, Z., Measuring Polymer Surface Ordering Differences in Air and Water by Sum Frequency Generation Vibrational Spectroscopy. *Journal of the American Chemical Society* **2002,** *124* (24), 7016-7023.
39. Wang, J.; Woodcock, S. E.; Buck, S. M.; Chen, C.; Chen, Z., Different Surface-Restructuring Behaviors of Poly(methacrylate)s Detected by SFG in Water. *Journal of the American Chemical Society* **2001,** *123* (38), 9470-9471.
40. Leng, C.; Sun, S.; Zhang, K.; Jiang, S.; Chen, Z., Molecular Level Studies on Interfacial Hydration of Zwitterionic and Other Antifouling Polymers In Situ. *Acta Biomaterialia* **2016,** *40*, 6-15.
41. Xiaokong, L.; Chuan, L.; Li, Y.; Ke, H.; Joan, B. L.; Zhan, C.; Jinhan, C.; Dayang, W., Ion-Specific Oil Repellency of Polyelectrolyte Multilayers in Water: Molecular Insights into the Hydrophilicity of Charged Surfaces. *Angewandte Chemie International Edition* **2015,** *54* (16), 4851-4856.
42. Callow, J.; Callow, M.; Ista, L.; Lopez, G.; Chaudhury, M., The Influence of Surface Energy on the Wetting Behaviour of the Spore Adhesive of the Marine Alga Ulva linza (synonym Enteromorpha linza). *Journal of the Royal Society Interface* **2005,** *2* (4), 319-325.
43. Thome, I.; Pettitt, M. E.; Callow, M. E.; Callow, J. A.; Grunze, M.; Rosenhahn, A., Conditioning of Surfaces by Macromolecules and its Implication for the Settlement of Zoospores of the Green Alga Ulva linza. *Biofouling* **2012,** *28* (5), 501-510.
44. Jung, S.-Y.; Lim, S.-M.; Albertorio, F.; Kim, G.; Gurau, M. C.; Yang, R. D.; Holden, M. A.; Cremer, P. S., The Vroman Effect: A Molecular Level Description of Fibrinogen Displacement. *Journal of the American Chemical Society* **2003,** *125* (42), 12782-12786.
45. Helmut, L.; Vance, J.; Lars, S.; Mischa, B.; Jim, P.; Tobias, W., The Structure of the Diatom Silaffin Peptide R5 within Freestanding Two-Dimensional Biosilica Sheets. *Angewandte Chemie International Edition* **2017,** *56* (28), 8277-8280.
46. Samson, J.-S.; Scheu, R.; Smolentsev, N.; Rick, S. W.; Roke, S., Sum Frequency Spectroscopy of the Hydrophobic Nanodroplet/Water Interface: Absence of Hydroxyl Ion and Dangling OH Bond Signatures. *Chemical Physics Letters* **2014,** *615*, 124-131.
47. Junjun, T.; Baixiong, Z.; Yi, L.; Shuji, Y., Ultrafast Vibrational Dynamics of Membrane-Bound Peptides at the Lipid Bilayer/Water Interface. *Angewandte Chemie International Edition* **2017,** *56* (42), 12977-12981.
48. Ding, B.; Jasensky, J.; Li, Y.; Chen, Z., Engineering and Characterization of Peptides and Proteins at Surfaces and Interfaces: A Case Study in Surface-Sensitive Vibrational Spectroscopy. *Accounts of Chemical Research* **2016,** *49* (6), 1149-1157.
49. Raschke, M. B.; Shen, Y. R., Nonlinear Optical Spectroscopy of Solid Interfaces. *Current Opinion in Solid State and Materials Science* **2004,** *8* (5), 343-352.
50. Gragson, D. E.; Richmond, G. L., Probing the Structure of Water Molecules at an Oil/Water Interface in the Presence of a Charged Soluble Surfactant through Isotopic Dilution Studies. *The Journal of Physical Chemistry B* **1998,** *102* (3), 569-576.
51. Uosaki, K.; Yano, T.; Nihonyanagi, S., Interfacial Water Structure at As-Prepared and UV-Induced Hydrophilic TiO2 Surfaces Studied by Sum Frequency Generation Spectroscopy

and Quartz Crystal Microbalance. *The Journal of Physical Chemistry B* **2004,** *108* (50), 19086-19088.
52. Du, Q.; Freysz, E.; Shen, Y. R., Surface Vibrational Spectroscopic Studies of Hydrogen Bonding and Hydrophobicity. *Science* **1994,** *264* (5160), 826.
53. Strazdaite, S.; Versluis, J.; Backus, E. H. G.; Bakker, H. J., Enhanced Ordering of Water at Hydrophobic Surfaces. *The Journal of Chemical Physics* **2014,** *140* (5), 054711.
54. Ochsenhirt, S. E.; Kokkoli, E.; McCarthy, J. B.; Tirrell, M., Effect of RGD Secondary Structure and the Synergy Site PHSRN on Cell Adhesion, Spreading and Specific Integrin Engagement. *Biomaterials* **2006,** *27* (20), 3863-3874.